

Lyapunov Design for Robust and Efficient Robotic Reinforcement Learning

Tyler Westenbroek^{1,*}
westenbroekt@berkeley.edu

Fernando Castañeda^{2,*}
fcastaneda@berkeley.edu

Ayush Agrawal^{2,*}
ayush.agrawal@berkeley.edu

Shankar Sastry¹
sastry@coe.berkeley.edu

Koushil Sreenath²
koushils@berkeley.edu

¹Department of Electrical Engineering and Computer Science, UC Berkeley

²Department of Mechanical Engineering, UC Berkeley

* Equal Contribution *

Abstract: Recent advances in the reinforcement learning (RL) literature have enabled roboticists to automatically train complex policies in simulated environments. However, due to the poor sample complexity of these methods, solving reinforcement learning problems using real-world data remains a challenging problem. This paper introduces a novel cost-shaping method which aims to reduce the number of samples needed to learn a stabilizing controller. The method adds a term involving a control Lyapunov function (CLF) – an ‘energy-like’ function from the model-based control literature – to typical cost formulations. Theoretical results demonstrate the new costs lead to stabilizing controllers when smaller discount factors are used, which is well-known to reduce sample complexity. Moreover, the addition of the CLF term ‘robustifies’ the search for a stabilizing controller by ensuring that even highly sub-optimal policies will stabilize the system. We demonstrate our approach with two hardware examples where we learn stabilizing controllers for a cartpole and an A1 quadruped with only seconds and a few minutes of fine-tuning data, respectively.



Figure 1: We learn precise policies on hardware for the Quanser cartpole [1] (top) and the Unitree A1 quadruped [2] (bottom) using only seconds and a few minutes of real-world data, respectively.

*This work was supported in part by NSF Grants CMMI-1944722 and CMMI-1931853. The work of Fernando Castaneda was partially supported through a fellowship from Fundacion Rafael del Pino, Spain. This work was supported by LOGiCS (Learning-Driven Oracle-Guided Compositional Symbiotic Design of Cyber-Physical Systems), Defense Advanced Research Projects Agency award number FA8750-20-C-0156.

1 Introduction

Recent years have witnessed many success stories for reinforcement learning (RL)-based controllers which are trained using massive amounts of simulation data. The primary obstacle for controller design methods which are based on a nominal dynamics model (including traditional ‘model-based’ methods) is the ‘reality gap’ between the simulation environment and the real-world system. This discrepancy occurs because it is generally impractical to model every facet of a real robotic system. This has led to the use of techniques such as domain randomization [3, 4], which attempt to robustify the trained controller by adding random perturbations to the simulated dynamics. Another approach is domain adaptation [5], which trains controllers over a distribution of unknown dynamics parameters and then attempts to identify the ‘true’ parameters online. In the last few years, these methods have been key ingredients in a number of impressive hardware results [6, 7, 8, 3, 9, 10].

However, despite these successes, there has been a renewed effort to incorporate data from hardware experiments into RL pipelines [11]. These two approaches are not at odds, as ‘fine-tuning’ [12, 13, 14, 15] approaches can be used to improve a policy initially trained on a simulation model. This is an ideal middle ground which enables engineers to incorporate known features of the system into the model while still allowing model-free methods to improve performance by leveraging complex unknown nonlinearities in the environment. However, the poor sample complexity of RL methods still presents an obstacle, as learning optimal policies can require significant amounts of data.

One of the key parameters in RL problems is the *discount factor*, which controls the effect that long-horizon behaviors have on the overall cost function. Theoretical and empirical results [16] have demonstrated that problems with large discount factors are significantly more challenging to solve. The standard approach to synthesizing stabilizing control policies with RL (and also model-based optimal control approaches [17]) is to simply penalize the distance of the state from the desired operating point. Unfortunately, costs of this form typically require using a high discount factor to learn a stabilizing policy [18, 17]. This is because stabilization is an inherently long-horizon behavior and, when costs of this form are used, the agent must plan over long horizons to see the benefits of stabilizing the system (rather than simply minimizing control effort).

This paper introduces a cost-shaping framework which aims to reduce the sample complexity of learning stabilizing control policies. Our method adds a term involving an (approximate) *control Lyapunov function* (CLF) for the system to the traditional cost formulations discussed above. CLFs are tools from the model-based control literature which are generalized ‘energy functions’ for the system. Any control law which decreases the value of the CLF at each time-step can be guaranteed to stabilize the system. Thus, CLFs reduce the long-horizon objective of stabilizing the system to a simple one-step condition. The CLF term we add to the cost function rewards actions which decrease the CLF over time, and thus incentivizes policies which stabilize the system. We provide a formal stability analysis which demonstrates that the new cost functions lead to stabilizing control policies, even when small discount factors are used and the learned policy is highly suboptimal.

We illustrate the effectiveness of our cost-shaping technique in three distinct contexts. In our hardware experiments for the cartpole and A1, initial policies are constructed using a nominal dynamics model and then improved using fine-tuning data from the real-world system. For the A1 experiment, the nominal controller is a model-based control architecture [19] and we use a CLF which is hand-designed around the desired trotting gait. For the cartpole swing-up task, it is much more difficult to hand-design a CLF for the desired task. Thus, we first train a RL policy for the task using the soft actor-critic algorithm [20] in simulation. We then use the value function learned during the initial training as a CLF for our fine tuning experiments. We discuss why the learned value function is a reasonable CLF for the system in Section 2.2. For both of our hardware experiments we rapidly learn stabilizing controllers by solving problems with small discount factors. Finally, with a toy simulation example of an inverted pendulum we demonstrate how our method can still accelerate learning by using moderate values of discount factors even when the proposed CLF used in our formulation is very crude.

1.1 Related Work

We outline how our approach departs from related work; Appendix A contains further discussion. **Discount Factors, Sample Complexity and Reward Shaping:** It is well-understood that the discount factor has a significant effect on the size of the data set that RL algorithms need to achieve a desired level of performance. Specifically, it has been shown in numerous contexts [21, 22, 23, 24] that smaller discount factors lead to problems which can be solved more efficiently. This has led to

a number of works which explicitly treat the discount factor as a parameter which can be used to control the complexity of the problem alongside reward shaping techniques [25, 26, 16, 27, 28, 29]. Compared to these works, our primary contribution is to demonstrate how CLFs can be combined with model-free algorithms to rapidly learn stabilizing controllers for robotic systems.

Fine-tuning with Real World Data: Recently, there has been much interest in using RL to fine-tune policies which have been pre-trained in simulation [12, 13, 14, 15]. These methods typically optimize the same cost function with a large discount factor in both simulation and on the real robot. In contrast, using our cost reshaping techniques, we solve a different problem with a smaller discount factor on hardware which can be solved more efficiently. In Appendix D, we show that our method outperforms typical fine-tuning approaches under moderate perturbations to the dynamics model.

Learning with Control Lyapunov Functions: A number of recent works have also tried to overcome the reality gap by using data-driven methods to improve CLF-based controllers [30, 31, 32, 33, 34, 35]. While these methods work very well when a true CLF for the real world system is available, our method is more general as we can still efficiently learn stabilizing controllers when only an approximate CLF is available by modulating the discount factor used to optimize our cost.

2 Background and Problem Setting

Throughout the paper we will consider deterministic discrete-time systems of the form:

$$x_{k+1} = F(x_k, u_k), \quad (1)$$

where $x_k \in \mathcal{X} \subset \mathbb{R}^n$ is the state at time k , $u_k \in \mathcal{U} \subset \mathbb{R}^m$ is the input applied to the system at that time, and $F: \mathcal{X} \times \mathcal{U} \rightarrow \mathbb{R}^n$ is the transition function for the system. This general nonlinear model is broad enough to cover many important continuous control tasks for robotics. We will let Π denote the space of all control policies $\pi: \mathcal{X} \rightarrow \mathcal{U}$ for the system.

2.1 Control Lyapunov Functions

Control Lyapunov functions [36, 37, 38, 39] are ‘energy-like’ functions for the dynamics (1). When a CLF is available it greatly simplifies the search for an asymptotically stabilizing policy for the system. This is because, while asymptotic stability is an infinite-horizon property, CLFs reduce the search for a stabilizing policy to a set of greedy one-step criteria. We review the notion of asymptotic stability in Appendix B for unfamiliar readers.

Definition 1. We say that a positive definite function $W: \mathbb{R}^n \rightarrow \mathbb{R}$ is a control Lyapunov function (CLF) for (1) if the following condition holds for each $x \in \mathcal{X} \setminus \{0\}$:

$$\min_{u \in \mathcal{U}} W(F(x, u)) - W(x) < 0. \quad (2)$$

The condition (2) ensures that for each $x \in \mathcal{X}$ there exists a choice of input which decreases the ‘energy’ $W(x)$. Any policy which satisfies the one-step condition $W(F(x, \pi(x))) - W(x) < 0$ can be guaranteed to asymptotically stabilize the system [40]. Given a CLF for the system, model-based methods constructively synthesize a controller which satisfies this property using either closed-form equations [37] or by solving an online (convex) optimization problem [41, 39] to satisfy (2).

Remark 1. (Designing Control Lyapunov Functions) While there is no general procedure for designing CLFs by hand for general nonlinear systems, there do exist constructive procedures for designing CLFs for many important classes of robotic systems, such as manipulator arms [38] and robotic walkers [39] using structural properties of the system. However, even in these cases, the CLF is typically designed ignoring constraints on the inputs and thus is only a local CLF (such as in the inverted pendulum example we consider in Section 4). In cases where it is too difficult to design a CLF by hand for the desired task, such as in the cartpole swing-up example we consider in Section 4, we demonstrate how to learn a CLF using a simulation environment.

Remark 2. (Effects of Model Uncertainty) An additional complication arises when there is a discrepancy between the dynamics of the real robot and the model used to design the CLF. Fortunately, CLFs are known to be robust under moderate dynamics perturbations [42, 30].

2.2 Stability of Dynamic Programming and Reinforcement Learning

Here we review how ‘typical’ choices of cost functions found in the literature can be used to learn stabilizing controllers. These results are from the dynamic-programming literature, and will serve as a point of comparison for the stability and robustness properties of our method. In particular, we

first consider a running cost $\ell: \mathcal{X} \times \mathcal{U} \rightarrow \mathbb{R}$ of the form $\ell(x, u) = Q(x) + R(u)$, where $Q: \mathcal{X} \rightarrow \mathbb{R}$ is the state cost and $R: \mathcal{U} \rightarrow \mathbb{R}$ is the input. Both Q and R are assumed to be positive definite functions (in practice, both are usually quadratic functions). Given a policy $\pi \in \Pi$, discount factor $\gamma \in [0, 1]$, and initial condition $x_0 \in \mathcal{X}$ the associated long-run cost is:

$$V_\gamma^\pi(x_0) = \sum_{k=0}^{\infty} \gamma^k \ell(x_k, \pi(x_k)) \quad (3)$$

s.t. $x_{k+1} = F(x_k, \pi(x_k))$,

where $V_\gamma^\pi: \mathcal{X} \rightarrow \mathbb{R} \cup \{\infty\}$ is the *value function* associated to π . Small discount factors incentivize policies which greedily optimize a small number of time steps into the future, while larger discount factors promote policies which reduce the cost in the long-run. We say that a policy $\pi_\gamma^* \in \Pi$ is *optimal* if it achieves the smallest cost from each $x \in \mathcal{X}$:

$$V_\gamma^{\pi_\gamma^*}(x) = V_\gamma^*(x) := \inf_{\pi \in \Pi} V_\gamma^\pi(x), \quad \forall x \in \mathcal{X}, \quad (4)$$

where $V_\gamma^*: \mathcal{X} \rightarrow \mathbb{R} \cup \{\infty\}$ is the *optimal value function*. Together V_γ^* and π_γ^* capture the ‘ideal’ behavior induced by the cost function (3). Unfortunately, it is impractical to search over the space of all policies Π . This necessitates the use of function approximation schemes (e.g. feed-forward neural networks) to instead represent a subset of policies $\hat{\Pi} \subset \Pi$ to search over. Indeed, modern RL approaches for robotics randomly sample the space of trajectories to optimize problems of the form:

$$\inf_{\pi \in \hat{\Pi}} \mathbb{E}_{x_0 \sim X_0} [V_\gamma^\pi(x_0)], \quad (5)$$

where X_0 is a distribution over initial conditions. While this approach enables these methods to optimize high-dimensional policies, they are data-hungry, can display high-variance and thus frequently return highly sub-optimal policies when data is limited. To better understand the effect that this has on the stability of learned policies, for each $\pi \in \hat{\Pi}$ define the *optimality gap*:

$$\epsilon_\gamma^\pi(x) = V_\gamma^\pi(x) - V_\gamma^*(x), \quad (6)$$

and recall that from (3), for each $x \in \mathcal{X}$ the policy satisfies the difference equation:

$$V_\gamma^\pi(x) = \gamma V_\gamma^\pi(F(x, \pi(x))) + \ell(x, \pi(x)). \quad (7)$$

From these equations we can obtain:

$$V_\gamma^\pi(F(x, \pi(x))) - V_\gamma^\pi(x) = \frac{1}{\gamma} (-\ell(x, \pi(x)) + (1 - \gamma)V_\gamma^\pi(x)) \quad (8)$$

$$= \frac{1}{\gamma} (-\ell(x, \pi(x)) + (1 - \gamma)[V_\gamma^*(x) + \epsilon_\gamma^\pi(x)]) \quad (9)$$

$$\leq \frac{1}{\gamma} (-Q(x) + (1 - \gamma)[V_\gamma^*(x) + \epsilon_\gamma^\pi(x)]), \quad (10)$$

where we have first rearranged (7), then used $V_\gamma^\pi(x) = V_\gamma^*(x) + \epsilon_\gamma^\pi(x)$, and finally we have used $\ell(x, \pi(x)) \geq Q(x)$. Inequalities of this sort are the building block for proving the stability of suboptimal policies in the dynamic programming literature [17, 18].

Remark 3. (*Value Functions as CLFs*) By inspecting the cost (3) we see that V_γ^π is positive definite (since Q is positive definite). Thus, if the right-hand side of (10) is negative for each $x \in \mathcal{X} \setminus \{0\}$, this inequality shows that V_γ^π is a CLF for (1), and that π is an asymptotically stabilizing control policy. In other words, V_γ^π is a CLF which is implicitly learned during the training process. Indeed, many RL algorithms directly learn an estimate of the value function, a fact which we later exploit to learn a CLF for the cartpole swing up-task in Section 4 using the nominal simulation environment, which is then used for fine-tuning a learned controller with real-world data.

Note that the RHS of (10) will only be negative if $V_\gamma^*(x) + \epsilon_\gamma^\pi(x) < \frac{1}{1-\gamma}Q(x)$ for each $x \in \mathcal{X}$. Since from (3) we know that $V_\gamma^*(x) > Q(x)$ for each $x \in \mathcal{X}$, even the optimal policy (which has no optimality gap) will only be stabilizing if γ is large enough. On the other hand, for a fixed $\gamma \in (0, 1]$, this inequality also explains how sub-optimal a policy can be while maintaining stability.

To make these observations more quantitative we make the following assumptions:

Assumption 1. *There exists $C \geq 1$ such that $V_\gamma^*(x) \leq CQ(x)$ for each $\gamma \in [0, 1]$ and $x \in \mathcal{X}$.*

Assumption 2. *There exists $\delta > 0$ such that the optimality gap for the policy $\pi \in \hat{\Pi}$ satisfies the bound $\epsilon_\gamma^\pi(x) \leq \delta Q(x)$ for each $x \in \mathcal{X}$ and a desired discount factor $\gamma \in (0, 1]$.*

Growth conditions of this form are standard in the literature on the stability of approximate dynamic programming [43, 18, 17, 44]. Noting that $V_\gamma^*(x) \leq V_{\gamma=1}^*(x)$ for each $\gamma \in [0, 1)$, the constant $C \geq 1$ upper-bounds the ratio between the one-step cost and the optimal undiscounted value function. Growth assumptions of this type are common in the approximate dynamic programming literature, and, generally speaking, the smaller the upper-bound $V_\gamma^*(x) \leq CQ(x)$ the more rapidly the methods converge to a stabilizing controller [43]. Assumption 2 provides a measure of how suboptimal the chosen policy is when compared to one-step of the state-cost. The following result is essentially a specialization of the main result from [44]:

Proposition 1. *Let Assumption 1 hold. Let $\pi \in \hat{\Pi}$ be a policy which satisfies Assumption 2 for discount factor $\gamma \in (0, 1]$. Then, π asymptotically stabilizes (1) if $C + \delta < \frac{1}{1-\gamma}$.*

Proof. Combining Assumptions 1 and 2 with equation (10) yields:

$$\gamma V_\gamma^\pi(F(x, \pi(x))) - \gamma V_\gamma^\pi(x) \leq (-1 + (1 - \gamma)[C + \delta])Q(x) \quad (11)$$

Note that if $C + \delta < \frac{1}{1-\gamma}$ then the right hand side of (11) will be negative definite, which establishes that π asymptotically stabilizes the system. \square

Remark 4. (*Stability Properties of Cost Function*) *In the following section we will derive an analogous result to Proposition 1 for the novel reshaped cost function we propose below. When comparing these results we will primarily focus on the effect of the constant $C \geq 1$ (and the equivalent constant for the new setting). This constant provides an estimate for the size of discount factor that is needed to stabilize (1) when the cost (3) is used. In particular, the discount factor must satisfy $\frac{1}{1-\gamma} > C$ to guarantee stability. The constant C also characterizes how ‘robust’ the cost function is to suboptimal policies. In particular, for a fixed discount factor, the policy will stabilize the system if $\delta < \frac{1}{1-\gamma} + C$, thus smaller values of C permit more suboptimal policies.*

3 Lyapunov Design for Infinite Horizon Reinforcement Learning

Our method uses a candidate control Lyapunov function $W: \mathbb{R}^n \rightarrow \mathbb{R}$ for the nonlinear dynamics (1), and reshapes (3) to our proposed new long horizon cost $\tilde{V}_\gamma^\pi: \mathcal{X} \rightarrow \mathbb{R} \cup \{\infty\}$:

$$\tilde{V}_\gamma^\pi(x_0) = \sum_{k=0}^{\infty} \gamma^k \left([W(F(x_k, \pi(x_k))) - W(x_k)] + \ell(x_k, \pi(x_k)) \right) \quad (12)$$

s.t. $x_{k+1} = F(x_k, \pi(x_k))$.

Here the term ‘candidate’ means that we guess that W is a CLF for the system. As we shall see below, our method works best when W is in fact a CLF for the system, but still provides benefits when it is only an ‘approximate’ CLF for the system (in a sense we will make precise later).

Given the reshaped cost, we then solve the following policy optimization problem:

$$\inf_{\pi \in \hat{\Pi}} \mathbb{E}_{x_0 \sim X_0} [\tilde{V}_\gamma^\pi(x_0)]. \quad (13)$$

The new cost function (12) includes the amount that W changes at each time step, and thus encourages choices of inputs which decrease W over time. For very small discount factors, the new cost biases the policy search in (13) towards policies which myopically decrease the value of W at each step. To see this, note that in the extreme case where $\gamma = 0$ we can simplify the cost to:

$$\tilde{V}_0^\pi(x_0) = W(F(x_0, \pi(x_0))) - W(x_0) + Q(x_0) + R(\pi(x_0)). \quad (14)$$

Since the policy cannot affect the initial condition $x_0 \in \mathbb{R}$, the only terms in (14) which affect the policy optimization (13) are $W(F(x, \pi(x)))$ and $R(\pi(x))$. Thus, optimal policies will disregard the original state cost Q , and myopically balance decreasing W against the input cost R . On the other hand, when γ is large, optimal policies can increase the value of W in the short run, if it means that W and Q can both be decreased in the long-run. The new optimal value function is given by:

$$\tilde{V}_\gamma^*(x) = \inf_{\pi \in \hat{\Pi}} \tilde{V}_\gamma^\pi(x), \quad (15)$$

and each policy must now satisfy the new difference equation:

$$\tilde{V}_\gamma^\pi(x) = \gamma \tilde{V}_\gamma^\pi(F(x, \pi(x))) + W(F(x, \pi(x))) - W(x) + \ell(x, \pi(x)). \quad (16)$$

In our stability analysis we will use the following composite function as a candidate CLF for (1):

$$\tilde{\mathbf{V}}_\gamma^\pi(x) = W(x) + \gamma \tilde{V}_\gamma^\pi(x). \quad (17)$$

We provide an interpretation of this curious candidate CLF in Remark 5 below, but first perform an initial analysis similar to the one presented in the previous section. Defining for each $\pi \in \hat{\Pi}$ and $x \in \mathcal{X}$ the new optimality gap:

$$\tilde{\epsilon}_\gamma^\pi(x) = \tilde{V}_\gamma^*(x) - \tilde{V}_\gamma^\pi(x), \quad (18)$$

and following steps analogous to those taken in (8)-(10), we can obtain the following:

$$\tilde{\mathbf{V}}_\gamma^\pi(F(x, \pi(x))) - \tilde{\mathbf{V}}_\gamma^\pi(x) = -\ell(x, \pi(x)) + (1 - \gamma)\tilde{V}_\gamma^\pi(x) \quad (19)$$

$$= -\ell(x, \pi(x)) + (1 - \gamma)[\tilde{V}_\gamma^*(x) + \tilde{\epsilon}_\gamma^\pi(x)] \quad (20)$$

$$\leq -Q(x) + (1 - \gamma)[\tilde{V}_\gamma^*(x) + \tilde{\epsilon}_\gamma^\pi(x)]. \quad (21)$$

Similar to the analysis in the previous section, we will aim to understand when the right hand side of (21) is negative, as this will characterize when π stabilizes the system. One key difference between the inequality (10) and (21) is that, while the original value function V_γ^* is necessarily positive definite, \tilde{V}_γ^* can actually take on negative values since the addition of the CLF term allows the new running cost in (12) to be negative. As we shall see, this forms the basis for the stability and robustness properties our cost formulation enjoys when W is designed properly.

Remark 5. (*Learning Corrections to W*) Even though \tilde{V}_γ^π can take on negative values, in Lemma 2 in the appendix we demonstrate that $\tilde{\mathbf{V}}_\gamma^\pi = W + \gamma \tilde{V}_\gamma^\pi$ is a positive definite function. Thus, when the right hand side of (21) is negative for each $x \in \mathcal{X} \setminus \{0\}$, inequality (21) demonstrates that $\tilde{\mathbf{V}}_\gamma^\pi$ is in fact a CLF for (1) and that π stabilizes the system. We can think of W as an ‘initial guess’ for a CLF for the system, while $\gamma \tilde{V}_\gamma^\pi$ is a ‘correction’ to W that is implicitly made by a learned policy π . Roughly speaking, the larger the discount factor, the larger this correction. Thus the user can trade-off how much the learned policy is able to correct the candidate CLF W against the additional complexity of solving a problem with a higher discount factor, depending on how good of a CLF candidate W is believed to be for the real robot.

We first state a general stability result for suboptimal policies associated to the new cost, and then discuss how the choice of W affects the stability of suboptimal control policies:

Assumption 3. *There exists $\tilde{C} \in \mathbb{R}$ such that $\tilde{V}_\gamma^*(x) \leq \tilde{C}Q(x)$ for each $\gamma \in [0, 1]$ and $x \in \mathcal{X}$.*

Assumption 4. *There exists $\tilde{\delta} > 0$ such that the optimality gap for the policy $\pi \in \hat{\Pi}$ satisfies the bound $\tilde{\epsilon}_\gamma^\pi(x) \leq \tilde{\delta}Q(x)$ for each $x \in \mathcal{X}$ and a desired discount factor $\gamma \in (0, 1]$.*

These Assumptions are entirely analogous to Assumptions 1 and 2, except in Assumption 3 the upper bound on the value function is allowed to take on negative values.

Theorem 1. *Let Assumption 3 hold. Let $\pi \in \hat{\Pi}$ be a policy which satisfies Assumption 4 for discount factor $\gamma \in (0, 1]$. Then π asymptotically stabilizes (1) if $\tilde{C} + \tilde{\delta} < \frac{1}{1-\gamma}$.*

The proof is conceptually similar to the proof of Proposition 1, and follows from the inequality (21) and Assumptions 3 and 4; we delegate the proof to Appendix C for brevity. Indeed, note that the conditions for stability under the new cost are essentially identical to those for the previous cost in Proposition 1. As alluded to in Remark 4, we will primarily focus on comparing how large the constants $C \geq 1$ and $\tilde{C} \in \mathbb{R}$ are for the two problems, as they control the discount factor required to learn a stabilizing policy and also the ‘robustness’ of the cost. The following result provides a condition on W which ensures that $\tilde{C} \leq 0$. This condition is from the model-predictive control literature [45, 46], which use CLFs as terminal costs. Proof can be found in Appendix C.

Lemma 1. *Suppose there exists $M \geq 0$ such that for each $x \in \mathcal{X}$ the following condition holds:*

$$\inf_{u \in U} W(F(x, u)) - W(x) + \ell(x, u) \leq -MQ(x). \quad (22)$$

Then Assumption 3 is satisfied with constant $\tilde{C} = -M$.

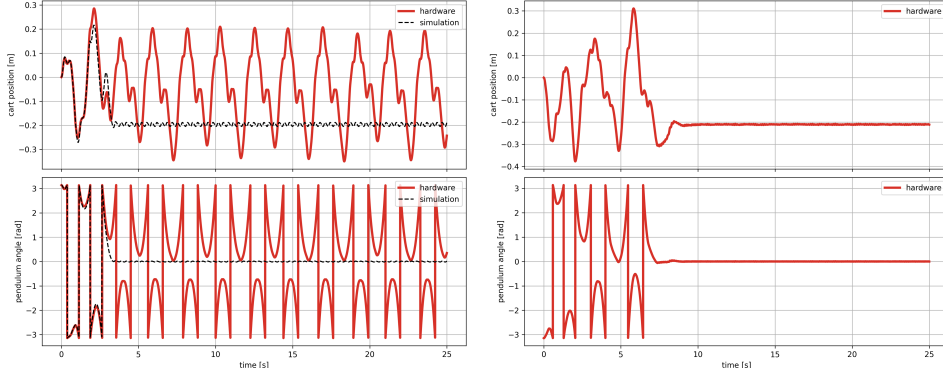


Figure 2: Experimental plots of the cart position and pendulum angle of the cartpole system. (left) The policy trained only in simulation fails to bring the real cartpole system to the upright position; (right) by fine-tuning the learned policy with 20s of real-world data using our CLF-based reward function, we obtain a successful policy.

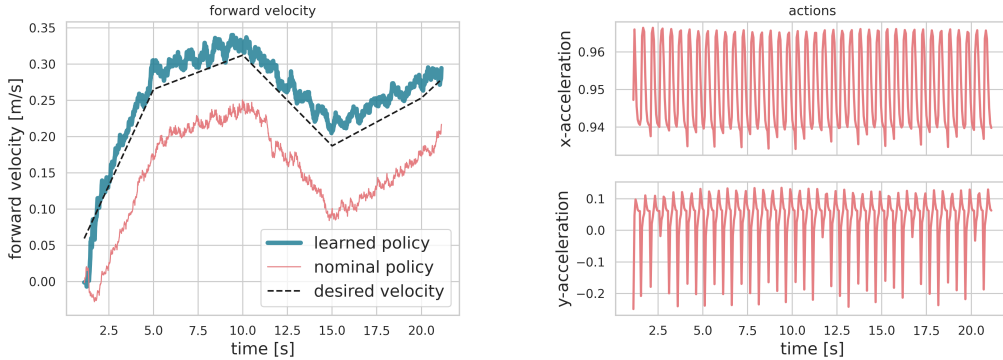


Figure 3: Experimental plots illustrating our proposed method to fine-tune a locomotion controller on the Unitree A1 robot hardware. (left) We illustrate improved velocity tracking of the learned policy (in dark green) compared to the nominal locomotion controller (in pink) to track a desired velocity profile (in dashed black line); (right) we show the normalized actions of the learned policy, which display a highly periodic profile which correlates strongly with individual walking steps.

Remark 6. (*Robustness of reshaped cost*) The condition in Lemma 1 implies that W is a CLF for the system which ‘dominates’ the original running cost ℓ , in the sense that at each time step W can be decreased faster than the running cost ℓ accumulates. In this case, we will have $\tilde{C} < C$ implying the new cost enjoys the desirable properties discussed above. Note that the constant $M > 0$ in Lemma 1 can be increased by putting more weight on W in the cost (12). In cases where W is only an ‘approximate’ CLF for the system, meaning that W cannot be decreased at each time step, but can instead be decreased over a window of a small number of time steps, \tilde{V}_γ^* may still take on negative values and contribute to the right hand side of (21) being negative. However, in this case moderate values of the discount factor may be needed to see these benefits, as policy optimization algorithms must implicitly plan further into the future to see the benefits of ‘going down’ W . The inverted pendulum example in Section 4 illustrates this point.

4 Examples and Practical Implementations

We highlight the main results for each of our examples, but leave certain details to Appendix D.

Fine-tuning a Learned Policy for Cartpole Swing-Up: We first fine-tune a swing-up controller for the Quanser cartpole system [1] using real world data and an initial policy which was pre-trained in simulation but that does not translate well to the real system. Due to the underactuated nature of the system, synthesizing a CLF, even when input constraints are ignored, is challenging. Thus, as alluded to previously, we use a ‘typical’ cost function of the form (3) and a discount factor of $\gamma = 0.999$ to learn a stabilizing neural network policy π_ϕ for a simulation model of the system using the SAC algorithm [47]. Given the discussion in Section 2.2, the value function V_θ associated with the learned policy will be a CLF for the simulation environment, and we use this as the candidate

CLF ($W = V_\theta$) in our reward reshaping formulation (12) for fine-tuning on hardware. In particular, when improving the simulation-based policy π_ϕ with real world data, we keep the parameters of this network fixed and learn an additional smaller policy π_ψ (so that the overall control action is produced by $\pi_\phi + \pi_\psi$) using our proposed CLF-based cost formulation. We solve the reshaped problem with a discount factor $\gamma = 0$ and collect rollouts of 10s on hardware. Our CLF-based fine-tuning approach is able to successfully complete the swing-up task after collecting data from just one rollout, however the behavior of the policy near the top is not smooth and sometimes fails. After collecting data from an additional rollout, the controller is much more reliable and robust enough to recover from several pushes. A successful swing-up motion is shown in Figure 2. Finally, in Appendix D, we compare our method with a typical fine-tuning approach which uses the same cost in both phases. We show that our method outperforms the baseline under moderate perturbations to the dynamics model.

Improving Velocity Tracking for a Quadruped Locomotion Controller: Next, we fine-tune a model-based trotting controller [19] for a quadruped robot walking at different speeds using a CLF which is designed around the desired gait. The tracking performance of this controller depends heavily on the chosen feedback gains. As illustrated by the pink curve in Fig. 3 (left), large steady-state errors persist when the controller is not well tuned. Furthermore, when the space of control parameters is large, tuning them by hand may not be straightforward. To address these limitations, we augment a policy π_ψ , to our nominal controller. To learn the parameters ψ , we first design a candidate CLF (W) based on a nominal linearized model of the robot, which is used to define our reward function. We then collect rollouts of 10s on the robot hardware with randomly chosen desired velocity profiles, and a discount factor $\gamma = 0$. Our approach is able to learn a policy which significantly improves the tracking performance of the nominal controller within 5 minutes (30 episodes) of hardware data. More details of this experiment are provided in Appendix D.

Inverted Pendulum with Input Constraints: Our final example demonstrates the utility of our method even when W is a crude guess for a CLF for the system, through the use of moderate discount factors. We illustrate this for a simple inverted pendulum by varying the magnitude of the input constraints for the system. We use the procedure from [39] to design a candidate CLF for the system. Like many CLF design techniques, this approach assumes there are no input constraints, and guides the pendulum to swing directly to the top. However, when the input constraints are too strict, this motion is infeasible and multiple pumps of the arm are required to swing upright. Thus, W is only a *local* CLF for the system, meaning it satisfies the CLF condition (2) only near the upright position. In the following simulations, we consider inputs bounds of the form $|u| \leq H$ for $H \in \{20, 7, 4\}$. For $H = 20$ the system has the control authority to swing directly to the top, while for $H = \{7, 4\}$ multiple pumping motions are required to gain enough momentum. Using the candidate CLF, we first train a stabilizing controller using a ‘typical’ cost function of the form (3), and then train a controller using the reshaped cost (12). For both forms of cost function, we sweep across different values of discount factor to approximately determine the smallest discount factor that can learn a stabilizing controller for each cost. In Figure 4, we display the training curves for the smallest discount factor which lead to a stabilizing controller (see Appendix D for details on how we determined if a controller is stabilizing). On each of the training curves the black dot denotes the first training epoch at which a stabilizing controller was obtained. As the plots clearly demonstrate, the addition of the CLF enables our method to more rapidly learn a stabilizing controller, but the effect is more pronounced when W is a better candidate CLF, namely when the input bound is larger. Moreover, in line with the presented theory, these results show that our method is able to more efficiently learn stabilizing policies with smaller discount factors.

5 Discussion and Limitations

As we have mentioned previously, our approach has several limitations. The cost shaping technique we introduce in Section 3 only provides benefits when W is in-fact a reasonable guess for a CLF for the true system. This requires that the user have a dynamics model which captures the primary features of the environments which affect the structure of CLFs for the system. While the cartpole simulations we provide in the Appendix D provide some intuition for when this will be the case, further research is needed to better understand in what scenarios we can see significant benefits from our method. Nonetheless, our two hardware experiments provide encouraging initial results which indicate that our method can rapidly learn stabilizing controllers using CLFs which are constructed using a nominal dynamics model. More broadly, there are many exciting avenues for further incorporating Lyapunov design techniques with RL, especially offline learning [11].

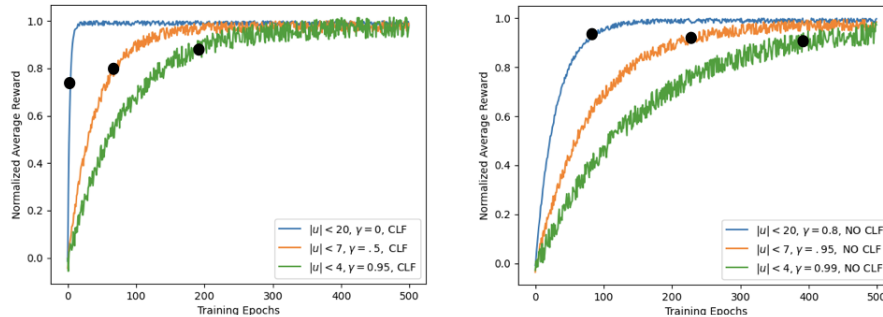


Figure 4: Learning curves for an inverted pendulum system under different input constraints. The curves plotted correspond to the smallest discount factors that led to stabilizing policies. On the left, the obtained learning curves use a CLF in the reward. On the right, the reward does not include the CLF term. The black dots denote the first stabilizing policy for each training.

References

- [1] Quanser. Linear servo base unit with inverted pendulum, Apr 2021. URL <https://www.quanser.com/products/linear-servo-base-unit-inverted-pendulum/>.
- [2] U. Robotics. A1. URL <https://www.unitree.com/products/a1/>.
- [3] X. B. Peng, M. Andrychowicz, W. Zaremba, and P. Abbeel. Sim-to-real transfer of robotic control with dynamics randomization. In *2018 IEEE international conference on robotics and automation (ICRA)*, pages 3803–3810. IEEE, 2018.
- [4] J. Tobin, R. Fong, A. Ray, J. Schneider, W. Zaremba, and P. Abbeel. Domain randomization for transferring deep neural networks from simulation to the real world. In *2017 IEEE/RSJ international conference on intelligent robots and systems (IROS)*, pages 23–30. IEEE, 2017.
- [5] D. Chen, B. Zhou, V. Koltun, and P. Krähenbühl. Learning by cheating. In *Conference on Robot Learning*, pages 66–75. PMLR, 2020.
- [6] J. Lee, J. Hwangbo, L. Wellhausen, V. Koltun, and M. Hutter. Learning quadrupedal locomotion over challenging terrain. *Science robotics*, 5(47), 2020.
- [7] A. Kumar, Z. Fu, D. Pathak, and J. Malik. Rma: Rapid motor adaptation for legged robots. *arXiv preprint arXiv:2107.04034*, 2021.
- [8] X. B. Peng, E. Coumans, T. Zhang, T.-W. Lee, J. Tan, and S. Levine. Learning agile robotic locomotion skills by imitating animals. *arXiv preprint arXiv:2004.00784*, 2020.
- [9] Z. Li, X. Cheng, X. B. Peng, P. Abbeel, S. Levine, G. Berseth, and K. Sreenath. Reinforcement learning for robust parameterized locomotion control of bipedal robots. *arXiv preprint arXiv:2103.14295*, 2021.
- [10] S. Belkhale, R. Li, G. Kahn, R. McAllister, R. Calandra, and S. Levine. Model-based meta-reinforcement learning for flight with suspended payloads. *IEEE Robotics and Automation Letters*, 6(2):1471–1478, 2021.
- [11] S. Levine, A. Kumar, G. Tucker, and J. Fu. Offline reinforcement learning: Tutorial, review, and perspectives on open problems. *arXiv preprint arXiv:2005.01643*, 2020.
- [12] L. Smith, J. C. Kew, X. B. Peng, S. Ha, J. Tan, and S. Levine. Legged robots that keep on learning: Fine-tuning locomotion policies in the real world. *arXiv preprint arXiv:2110.05457*, 2021.
- [13] R. Julian, B. Swanson, G. S. Sukhatme, S. Levine, C. Finn, and K. Hausman. Never stop learning: The effectiveness of fine-tuning in robotic reinforcement learning. *arXiv preprint arXiv:2004.10190*, 2020.

- [14] R. Julian, B. Swanson, G. S. Sukhatme, S. Levine, C. Finn, and K. Hausman. Efficient adaptation for end-to-end vision-based robotic manipulation. 2020.
- [15] Z. Mandi, P. Abbeel, and S. James. On the effectiveness of fine-tuning versus meta-reinforcement learning. *arXiv preprint arXiv:2206.03271*, 2022.
- [16] V. François-Lavet, R. Fonteneau, and D. Ernst. How to discount deep reinforcement learning: Towards new dynamic strategies. *arXiv preprint arXiv:1512.02011*, 2015.
- [17] V. Gaitsgory, L. Grüne, and N. Thatcher. Stabilization with discounted optimal control. *Systems & Control Letters*, 82:91–98, 2015.
- [18] R. Postoyan, L. Buşoniu, D. Nešić, and J. Daafouz. Stability analysis of discrete-time infinite-horizon optimal control with discounted cost. *IEEE Transactions on Automatic Control*, 62(6): 2736–2749, 2016.
- [19] X. Da, Z. Xie, D. Hoeller, B. Boots, A. Anandkumar, Y. Zhu, B. Babich, and A. Garg. Learning a contact-adaptive controller for robust, efficient legged locomotion. In *Conference on Robot Learning*, pages 883–894. PMLR, 2021.
- [20] T. Haarnoja, S. Ha, A. Zhou, J. Tan, G. Tucker, and S. Levine. Learning to walk via deep reinforcement learning. *arXiv preprint arXiv:1812.11103*, 2018.
- [21] D. P. Bertsekas and J. N. Tsitsiklis. *Neuro-dynamic programming*. Athena Scientific, 1996.
- [22] J. Schulman, F. Wolski, P. Dhariwal, A. Radford, and O. Klimov. Proximal policy optimization algorithms. *arXiv preprint arXiv:1707.06347*, 2017.
- [23] R. Munos and C. Szepesvári. Finite-time bounds for fitted value iteration. *Journal of Machine Learning Research*, 9(5), 2008.
- [24] R. Postoyan, M. Granzotto, L. Buşoniu, B. Scherrer, D. Nešić, and J. Daafouz. Stability guarantees for nonlinear discrete-time systems controlled by approximate value iteration. In *2019 IEEE 58th Conference on Decision and Control (CDC)*, pages 487–492. IEEE, 2019.
- [25] N. Jiang, A. Kulesza, S. Singh, and R. Lewis. The dependence of effective planning horizon on model accuracy. In *Proceedings of the 2015 International Conference on Autonomous Agents and Multiagent Systems*, pages 1181–1189. Citeseer, 2015.
- [26] M. Petrik and B. Scherrer. Biasing approximate dynamic programming with a lower discount factor. *Advances in neural information processing systems*, 21:1265–1272, 2008.
- [27] C. Tessler and S. Mannor. Reward tweaking: Maximizing the total reward while planning for short horizons. *arXiv preprint arXiv:2002.03327*, 2020.
- [28] C.-A. Cheng, A. Kolobov, and A. Swaminathan. Heuristic-guided reinforcement learning. *Advances in Neural Information Processing Systems*, 34:13550–13563, 2021.
- [29] A. Y. Ng, D. Harada, and S. Russell. Policy invariance under reward transformations: Theory and application to reward shaping. In *Icml*, volume 99, pages 278–287, 1999.
- [30] A. J. Taylor, V. D. Dorobantu, H. M. Le, Y. Yue, and A. D. Ames. Episodic learning with control lyapunov functions for uncertain robotic systems. In *2019 IEEE/RSJ International Conference on Intelligent Robots and Systems (IROS)*, pages 6878–6884. IEEE, 2019.
- [31] A. J. Taylor, V. D. Dorobantu, M. Krishnamoorthy, H. M. Le, Y. Yue, and A. D. Ames. A control lyapunov perspective on episodic learning via projection to state stability. In *2019 IEEE 58th Conference on Decision and Control (CDC)*, pages 1448–1455. IEEE, 2019.
- [32] T. Westenbroek, F. Castañeda, A. Agrawal, S. S. Sastry, and K. Sreenath. Learning min-norm stabilizing control laws for systems with unknown dynamics. In *2020 59th IEEE Conference on Decision and Control (CDC)*, pages 737–744. IEEE, 2020.

- [33] T. Westenbroek, A. Agrawal, F. Castañeda, S. S. Sastry, and K. Sreenath. Combining model-based design and model-free policy optimization to learn safe, stabilizing controllers. *IFAC-PapersOnLine*, 54(5):19–24, 2021.
- [34] F. Castañeda, J. J. Choi, B. Zhang, C. J. Tomlin, and K. Sreenath. Gaussian process-based min-norm stabilizing controller for control-affine systems with uncertain input effects and dynamics. In *2021 American Control Conference (ACC)*, pages 3683–3690, 2021.
- [35] J. Choi, F. Castañeda, C. Tomlin, and K. Sreenath. Reinforcement Learning for Safety-Critical Control under Model Uncertainty, using Control Lyapunov Functions and Control Barrier Functions. In *Robotics: Science and Systems*, Corvalis, OR, July 2020.
- [36] Z. Artstein. Stabilization with relaxed controls. *Nonlinear Analysis: Theory, Methods & Applications*, 7(11):1163–1173, 1983.
- [37] E. D. Sontag. A ‘universal’ construction of artstein’s theorem on nonlinear stabilization. *Systems and Control Letters*, 13(2):117 – 123, 1989.
- [38] A. D. Ames and M. Powell. Towards the unification of locomotion and manipulation through control lyapunov functions and quadratic programs. *Lecture Notes in Control and Information Sciences*, 449:219–240, 2013.
- [39] A. D. Ames, K. Galloway, K. Sreenath, and J. W. Grizzle. Rapidly exponentially stabilizing control lyapunov functions and hybrid zero dynamics. *IEEE Transactions on Automatic Control*, 59(4):876–891, 2014.
- [40] C. M. Kellett and A. R. Teel. Results on discrete-time control-lyapunov functions. In *42nd IEEE International Conference on Decision and Control (IEEE Cat. No. 03CH37475)*, volume 6, pages 5961–5966. IEEE, 2003.
- [41] R. Freeman and P. V. Kokotovic. *Robust nonlinear control design: state-space and Lyapunov techniques*. Springer Science and Business Media, 2008.
- [42] Y. S. Ledyayev and E. D. Sontag. A lyapunov characterization of robust stabilization. *Nonlinear Analysis: Theory, Methods & Applications*, 37(7):813–840, 1999.
- [43] B. Lincoln and A. Rantzer. Relaxing dynamic programming. *IEEE Transactions on Automatic Control*, 51(8):1249–1260, 2006.
- [44] V. Gaitsgory, L. Grüne, C. M. Kellett, and S. R. Weller. Stabilization with discounted optimal control: the discrete time case. 2016.
- [45] A. Jadbabaie, J. Yu, and J. Hauser. Receding horizon control of the caltech ducted fan: A control lyapunov function approach. In *Proceedings of the 1999 IEEE International Conference on Control Applications (Cat. No. 99CH36328)*, volume 1, pages 51–56. IEEE, 1999.
- [46] G. Grimm, M. J. Messina, S. E. Tuna, and A. R. Teel. Model predictive control: for want of a local control lyapunov function, all is not lost. *IEEE Transactions on Automatic Control*, 50(5):546–558, 2005.
- [47] T. Haarnoja, A. Zhou, P. Abbeel, and S. Levine. Soft actor-critic: Off-policy maximum entropy deep reinforcement learning with a stochastic actor. *CoRR*, abs/1801.01290, 2018.
- [48] A. Jadbabaie and J. Hauser. On the stability of receding horizon control with a general terminal cost. *IEEE Transactions on Automatic Control*, 50(5):674–678, 2005.
- [49] A. Jadbabaie, J. Yu, and J. Hauser. Unconstrained receding-horizon control of nonlinear systems. *IEEE Transactions on Automatic Control*, 46(5):776–783, 2001.
- [50] G. Grimm, M. J. Messina, S. E. Tuna, and A. R. Teel. Examples when nonlinear model predictive control is nonrobust. *Automatica*, 40(10):1729–1738, 2004.
- [51] S. Sastry. *Nonlinear systems: analysis, stability, and control*, volume 10. Springer Science & Business Media, 1999.
- [52] S. Gu, E. Holly, T. Lillicrap, and S. Levine. Deep reinforcement learning for robotic manipulation with asynchronous off-policy updates. In *2017 IEEE international conference on robotics and automation (ICRA)*, pages 3389–3396. IEEE, 2017.

A Additional Literature Review

Model Predictive Control We briefly review stability results from the model predictive control (MPC) literature, focusing our discussion on the benefits of using a CLF as the terminal cost. In their simplest form, MPC control schemes minimize a cost functional of the form

$$\begin{aligned} \inf_{\hat{\mathbf{u}} \in \mathcal{U}^N} J_{MPC}^N(x_k, \hat{\mathbf{u}}) &= \sum_{k=0}^{N-1} (Q(\hat{x}_k) + R(\hat{u}_k)) + \hat{W}(\hat{x}_N) \\ \text{s.t. } \hat{x}_{k+1} &= F(\hat{x}_k, \hat{u}_k), \quad \hat{x}_0 = x_k, \end{aligned}$$

where x_k is the current state of the real-world system, $N \in \mathbb{N}$ is the prediction horizon, $\{\hat{x}_k\}_{k=0}^N$ and $\hat{\mathbf{u}} = \{\hat{u}_k\}_{k=0}^{N-1} \in \mathcal{U}^N$ are a predictive state trajectory and control sequence, Q and R are as above, and $\hat{W}: \mathbb{R}^n \rightarrow \mathbb{R}_{\geq 0}$ is the terminal cost which is assumed to be a proper function. The MPC controller then applies the first step of the resulting open loop control and the process repeats, implicitly defining a control law $u_{MPC}(x)$. The MPC cost $J_{MPC}^N(x_k, \cdot)$ can be thought of as a finite-horizon approximation of the original cost (3) (except that it is defined over an open-loop sequence of control inputs instead of being a cost over policies).

Stability results from the MPC literature focus primarily on the effects of the prediction horizon N and the choice of terminal cost \hat{W} . Under mild conditions, for any choice of terminal cost (including $\hat{W}(\cdot) \equiv 0$), the user can guarantee that the MPC scheme stabilizes the system on any desired operating region by making the prediction horizon N sufficiently large [48, 46]. Thus, there is a clear connection between the explicit prediction horizon N in MPC schemes and the discount factor γ , as both need to be sufficiently large if a stabilizing controller is to be obtained (since trajectory optimization problems with longer time horizons are generally more difficult to solve). Indeed, in [18] it was pointed out that the *implicit prediction horizon* $\frac{1}{1-\gamma}$, a factor which shows up in the stability conditions in Proposition 1, plays essentially the same role in stability analysis as N for an MPC scheme with no terminal cost when the running cost is $\ell = Q + R$. Thus, much like the ‘typical’ policy optimization problems discussed in Section 2.2, MPC schemes with no terminal cost (or one which is chosen poorly) may require an excessively long prediction horizon to stabilize the system.

Fortunately, the MPC literature has a well-established technique for reducing the prediction horizon needed to stabilize the system: use an (approximate) CLF for the terminal cost \hat{W} [49, 48, 46]. Indeed, roughly speaking, these results guarantee that for *any prediction horizon* $N \in \mathbb{N}$ the MPC scheme will be stabilizing if \hat{W} is a valid CLF for the system. Extensive empirical evidence [45] and formal analysis [49] has demonstrated that well-designed CLF terminal costs reduce the prediction horizon needed to stabilize the system on a desired set and increase the robustness of the overall MPC control scheme [50]. Thus, in many ways our cost-resaping approach can be seen as a way to obtain these benefits in the context of infinite horizon model-free reinforcement learning.

B Asymptotic Stability and Lyapunov Theory

B.1 Asymptotic Stability and Lyapunov Theory

Next we briefly introduce the elements from stability theory and Lyapunov theory which we use extensively throughout the paper.

B.2 Notation and Terminology

We say that a function $W: \mathbb{R}^n \rightarrow \mathbb{R}$ is *positive definite* if $W(0) = 0$ and $W(x) > 0$ if $x \neq 0$. Let $\alpha: [0, \infty) \rightarrow [0, \infty)$ be a continuous function. We say that α is in class \mathcal{K} (denoted $\alpha \in \mathcal{K}$) if $\alpha(0) = 0$ and α is strictly increasing. If in addition we have $\alpha(r) \rightarrow \infty$ as $r \rightarrow \infty$ when we say that α is in class \mathcal{K}_∞ (denoted $\alpha \in \mathcal{K}_\infty$). Let $\beta: [0, \infty) \times [0, \infty)$ be a continuous function. We say that β is in class \mathcal{KL} if for each fixed $t \in [0, \infty)$ the function $\beta(\cdot, t)$ is in class \mathcal{K} and for each fixed $r \in [0, \infty)$ we have $\beta(r, t) \rightarrow 0$ as $t \rightarrow \infty$.

B.3 Basic Stability Results

Definition 2. We say that the closed loop system $x_{k+1} = F(x_k, \pi(x_k))$ is asymptotically stable on the set $D \subset \mathbb{R}^n$ if there exists $\beta \in \mathcal{KL}$ such that for each initial condition $x_0 \in D$ and $k \in \mathbb{N}$ the

closed-loop trajectory satisfies:

$$\|x_k\|_2 \leq \beta(\|x_0\|_2, k). \quad (23)$$

Analogously, if the preceding condition holds then we say that π asymptotically stabilizes (1).

In words, the definition says that π asymptotically stabilizes (1) if all trajectories of the closed-loop system $x_{k+1} = F(x_k, \pi(x_k))$ converge to the origin. Asymptotic stability is a difficult property to verify directly as it requires reasoning about the infinite-horizon behavior of trajectories. Lyapunov functions are a powerful analysis tool which can verify asymptotic stability with a ‘one-step’ criterion:

Definition 3. We say that the positive definite function $W : \mathbb{R}^n \rightarrow \mathbb{R}$ is a Lyapunov function for the closed-loop system $x_{k+1} = F(x_k, \pi(x_k))$ if for each $x \in \mathbb{R}^n$ we have:

$$W(F(x, \pi(x))) - W(x) < 0. \quad (24)$$

Intuitively, the Lyapunov function W can be thought of as an energy-like function for the closed loop system $x_{k+1} = F(x_k, \pi(x_k))$. In this light, the condition (24) ensures that the ‘energy’ of the closed-loop system is decreasing at each point in the state-space. This condition guarantees that the closed-loop system is asymptotically stable [51], and is a simple algebraic condition. Note that while control Lyapunov functions are defined formally for the open-loop dynamics (1), a Lyapunov function is defined for a particular set of closed-loop dynamics. That is, a control Lyapunov function W for $x_{k+1} = F(x_k, u_k)$ becomes a Lyapunov function for the closed-loop dynamics $x_{k+1} = F(x_k, \pi(x_k))$ after we apply a control law π which satisfies $W(F(x, \pi(x))) - W(x) < 0$ for each $x \in \mathcal{X}$.

C Missing Proofs and Intermediate Results

Lemma 2. The composite function $\tilde{\mathcal{V}}_\gamma^\pi = W + \gamma \tilde{V}_\gamma^\pi : \mathcal{X} \rightarrow \mathbb{R} \cup \{\infty\}$ is positive definite.

Proof. Note that we can re-write the reshaped cost (12) as

$$\tilde{V}_\gamma^\pi(x_0) = \sum_{k=0}^{\infty} \gamma^k \left([W(x_{k+1}) - W(x_k) + \ell(x_k, \pi(x_k))] \right), \quad (25)$$

where $\{x_k\}_{k=0}^{\infty}$ is the state trajectory generated by the policy π from the initial condition $x_0 \in \mathcal{X}$. By rearranging terms we can rewrite this expression as:

$$\tilde{V}_\gamma^\pi(x_0) = -W(x_0) + (1 - \gamma) \sum_{k=1}^{\infty} \gamma^k W(x_k) + \sum_{k=0}^{\infty} \gamma^k \ell(x_k, \pi(x_k)) > -W(x_0) + Q(x_0) \quad (26)$$

where we have used the fact that W and ℓ are both non-negative, and that $\ell(x_0, \pi(x_0)) > Q(x_0)$. Thus, using this expression we see that

$$\tilde{\mathcal{V}}_\gamma^\pi(x_0) = W(x_0) + \gamma \tilde{V}_\gamma^\pi(x_0) > (1 - \gamma)W(x_0) + \gamma Q(x_0), \quad (27)$$

Since Q and W are assumed to be positive definite functions this demonstrates that $\tilde{\mathcal{V}}_\gamma^\pi$ is in fact positive definite, since a convex combination of positive definite functions is positive definite. The proof is concluded by noting that the choice of γ and π is arbitrary, and thus the conclusion that $\tilde{\mathcal{V}}_\gamma^\pi$ is positive definite holds for all policies and discount factors. \square

C.1 Proof of Theorem 1

Proof. Lemma 2 demonstrates that $\tilde{\mathcal{V}}_\gamma^\pi = W + \gamma \tilde{V}_\gamma^\pi : \mathcal{X} \rightarrow \mathbb{R} \cup \{\infty\}$ is a positive definite function. Combining Assumptions 3 and 4 with the inequality (21) we obtain

$$\tilde{\mathcal{V}}_\gamma^\pi(F(x, \pi(x))) - \tilde{\mathcal{V}}_\gamma^\pi(x) \leq (-1 + (1 - \gamma)[\tilde{C} + \tilde{\delta}])Q(x). \quad (28)$$

Note that if $\tilde{C} + \tilde{\delta} < \frac{1}{1 - \gamma}$ then the right hand side of (11) will be negative definite, which establishes that π asymptotically stabilizes the system. \square

C.2 Proof of Lemma 1

Proof. In order to show the result we only need to show that there exists one policy for which $\tilde{V}_\gamma^\pi(x_0) < -MQ(x_0)$ from each initial condition. Consider a policy $\bar{\pi} \in \Pi$ defined for each $x \in \mathcal{X}$ by:

$$\bar{\pi}(x) \in \arg \inf_{u \in \mathcal{U}} W(F(x, u)) - W(x) + \ell(x, u) \leq -MQ(x), \quad (29)$$

where the preceding inequality follows directly from the assumptions made in the Lemma. Next, for a given initial condition $x_0 \in \mathcal{X}$ let $\{x_k\}_{k=0}^\infty$ be the state trajectory generated by $\bar{\pi}$. The corresponding reshaped cost is given by

$$\tilde{V}_\gamma^{\bar{\pi}}(x_0) = \sum_{k=0}^{\infty} \gamma^k \left([W(F(x_k, \bar{\pi}(x_k))) - W(x_k)] + \ell(x_k, \bar{\pi}(x_k)) \right) \quad (30)$$

$$\leq \sum_{k=0}^{\infty} \gamma^k (-MQ(x_k)) \quad (31)$$

$$\leq -MQ(x_0), \quad (32)$$

which demonstrates the desired result, since the initial condition and discount factor were chosen arbitrarily. \square

D Additional Experiment Details

We now provide more details of the experimental results reported in Section 4 and also additional evaluations. While we have chosen to minimize costs in the main portion of the paper, as this is more consistent with the notation used in the literature on Lyapunov theory and the stability of dynamic programming, most RL algorithms take in rewards that are to be maximized. Thus, for the sake of consistency with practical implementations, in this section we report the reward functions used in our code, which are simply the costs from before with the sign flipped.

D.1 Cartpole Results

We first give additional details about the cartpole experiments presented in Section 4, and then provide a comparison of the performance of our approach with respect to a typical fine-tuning method on the cartpole system.

Additional Details of Hardware Fine-Tuning Experiments:

For the experiments presented in Section 4, we used a Quanser Linear Servo Base Unit with Inverted Pendulum [1], with a pendulum length of 60cm. The system has 4 states, $x = [p, \alpha, \dot{p}, \dot{\alpha}] \in \mathbb{R}^4$, corresponding to the cart position p , the pendulum angle α , and their respective velocities. The control input is the voltage applied to the motor that actuates the cart $u \in \mathbb{R}$.

We first train a SAC agent in simulation using a ‘conventional’ RL reward that penalizes the distance to the equilibrium, control effort, and includes a penalty if the cart goes off-bounds $r(x_k, u_k) = -0.1(5\alpha_k^2 + p_k^2 + 0.05u_k^2) - 5 \cdot 10^3 \cdot \mathbb{1}(|p_k| \geq 0.3)$. The observations of the RL agent are state measurements, the actions are direct voltage commands with limits set to $|u| < 10V$ as specified by the manufacturer, and the simulation is run at 100Hz. In order to obtain a stabilizing swing-up policy with this traditional reward, a high discount factor is needed, so we use $\gamma = 0.999$. After around 10^4 seconds of simulation data with a learning rate of $5 \cdot 10^{-4}$, the RL agent learns to consistently swing-up and balance the pendulum at the upright position in simulation. However, when deployed on the cartpole hardware system, the policy from simulation fails to obtain successful swing-up behaviors due to the sim-2-real gap, as shown in the attached video.

To tackle these issues, we exploit the fact that SAC uses a feedforward neural network to approximate the discounted value function of the problem, and we use this approximate value function as a CLF candidate to fine-tune the learned policy directly on hardware.

Thus, we learn on hardware a fine-tuning policy u_ψ (MLP with 2 hidden layers of 64×64) whose actions are added to the ones of the policy trained on simulation u_ϕ (MLP with 2 hidden layers of 400×300). The action space limits for this new policy are set to $|u_\psi| < 4V$ but we still have a saturation of the total voltage $|u_\phi + u_\psi| < 10V$. The reward for this new policy is $\hat{r}(x_k, u_k) = \Delta V_\theta(x_k, u_k) - 0.1 \cdot (5\alpha_k^2 + p_k^2 + 0.05u_k^2)$, where V_θ is the value function network of the SAC agent that was trained in simulation. This allows us to set the discount factor $\gamma = 0$ for

the fine-tuning policy learned on hardware and therefore greatly reduce the difficulty of the learning problem. After only one episode of 10 seconds of real-world data we obtain a policy that manages to swing-up the pendulum to the upright position, and stabilizes it at the top. However, the behavior near the top is not smooth, and it fails for some different initial conditions. After training with another episode of 10 seconds of data, we obtain a policy that consistently manages to swing-up and balance the pendulum at the top, while the cart stays in-bounds. The plots in Figure 2(right) show the cart position and the pendulum angle when deploying the fine-tuned policy in the real Quanser cartpole system. The plots in Figure 2(left) show the results when using the policy that has been only trained in simulation, and how its performance is very different when deployed in simulation vs in hardware. A video with the results of the cartpole experiments has been submitted as additional material, and a sequence of snapshots of a successful experiment that uses the fine-tuned policy can be found in Figure 1.

For training from hardware data, we used asynchronous off-policy updates, similar to the framework presented in [52]. In particular, we have two separate threads, with one running episodes on the hardware system with the latest available policy and adding the transition data to the replay buffer, and the other one sampling from this buffer and performing the actor and critic updates. We only synchronize the policy network weights at the beginning of each episode. For the cartpole system, the episodes are 10 seconds long, and the policy is run at 500Hz, with each episode consisting of 5000 data points.

Comparison with a Typical Fine-Tuning Method:

As explained at the beginning of the paper, previous work has shown that using hardware data to fine-tune a policy that has been pre-trained in simulation is a powerful approach to tackle the sim-2-real gap problem (e.g. [12, 13, 14, 15]). These methods typically take the RL agent trained in simulation and continue its learning process using hardware data. In contrast, our proposed approach stops the simulation training of u_ϕ and learns a smaller offset policy u_ψ from hardware data using a separate learning process that has a different reward function \hat{r} (with the CLF candidate being the learned value function in simulation) and a smaller discount factor (in this case $\gamma = 0$).

In Figure 5, we explore how a typical fine-tuning method would perform in this cartpole swing-up task compared to our method. This comparison is done purely in simulation. We pre-train π_θ on a nominal dynamics model of the cartpole system until convergence to a stabilizing policy, using SAC and the reward $r(x_k, u_k) = -0.1(5\alpha_k^2 + p_k^2 + 0.05u_k^2) - 5 \cdot 10^3 \cdot \mathbb{1}(|p_k| \geq 0.3)$. Then, we modify the dynamics of the system by multiplying the weight and friction of the cart by 3 and by increasing the mass, inertia and length of the pendulum a 25%. After doing this, we randomly sample 10 initial conditions around the downright position ($-0.05m \leq p_0 \leq 0.05m$, $-\pi + 0.05rad \leq \alpha_0 \leq \pi - 0.05rad$, $-0.05m/s \leq \dot{p}_0 \leq 0.05m/s$, $-0.05rad/s \leq \dot{\alpha}_0 \leq 0.05rad/s$). We label a trial as success if within 10 seconds of simulation, the pendulum is stabilized in the set $-0.12rad < \alpha < 0.12rad$, $-0.3rad/s < \dot{\alpha} < 0.3rad/s$ and the cart never gets out of bounds ($|p| < 0.3$). The policy u_ϕ trained with data from the nominal dynamics model completely fails to swing-up and stabilize the dynamics of the new system and does not succeed for any of the 10 initial conditions. The baseline in Figure 5 is obtained by emptying the replay buffer and using new data to continue the training process of u_ϕ with the same reward $r(x_k, u_k)$ in the environment that has the new dynamics. On the other hand, as with the hardware experiments, our method takes the learned value function V_θ from the nominal dynamics model and learns an additional policy u_ψ using the modified reward $\hat{r}(x_k, u_k) = \Delta V_\theta(x_k, u_k) - 0.1 \cdot (5\alpha_k^2 + p_k^2 + 0.05u_k^2)$. We plot for 10 training random seeds, the average original reward $r(x_k, u_k)$ and the cumulative number of successes of the validation episodes ran from the initial conditions mentioned above. The x axis is the number of rollouts of fine-tuning data (each rollout consists of 10 seconds of data). It can be clearly seen that our method outperforms the baseline, achieving a high reward and success rate with less than 10 episodes of data. In fact, it is remarkable that our fine-tuning policy, being trained with a different reward function $\hat{r}(x_k, u_k)$, clearly outperforms the baseline when using the baseline’s own reward function $r(x_k, u_k)$ as metric.

The above results show that our approach effectively serves to fine-tune policies when the dynamics of the system change. In fact, we have artificially added a severe model mismatch and shown that we can adapt to the new dynamics with a discount factor of 0. This is because the original value function is still a ‘good’ CLF candidate for the new system. However, if the change in the dynamics is drastic, or if the overall shape of the motion required to complete the task has to be greatly modified, then the value function from the original dynamics may not be a good CLF candidate, and our method might fail. We have observed that for the cartpole example our method is very robust to

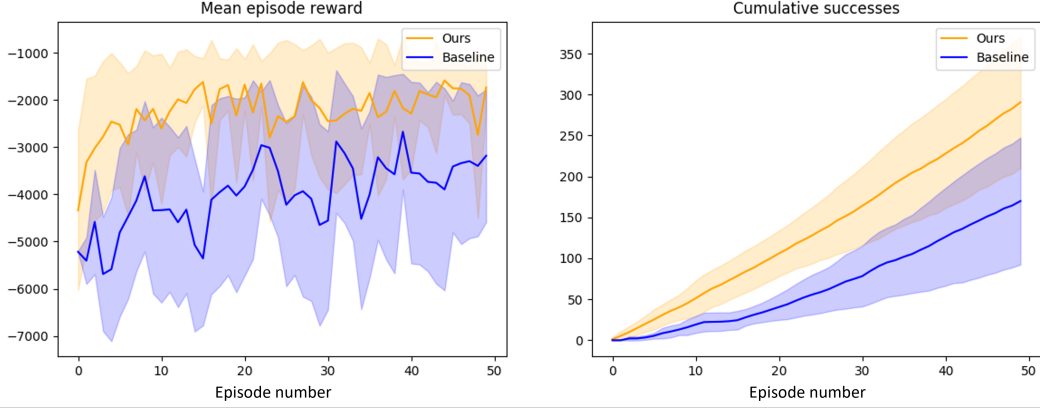


Figure 5: Comparison of the simulation results of fine-tuning a cartpole swing-up policy after adding a model mismatch. A policy trained on a nominal dynamics model of the cartpole fails when deployed on the new dynamics. In blue, we show the results of doing continual learning on the new dynamics with the original SAC agent (the replay buffer is emptied after changing the dynamics). In orange, we fine-tune using our method (learning an additional SAC agent trained with the CLF-based reward). For each episode of training on the new dynamics model, we compare the performance of both methods when running the cartpole from 10 validation initial conditions: (on the left) the average original reward without the CLF term $r(x_k, u_k) = -0.1(5\alpha_k^2 + p_k^2 + 0.05u_k^2) - 5 \cdot 10^3 \cdot \mathbb{1}(|p_k| \geq 0.3)$, and (on the right) the cumulative number of successful swing-ups. The plots show the mean and standard deviation of the results over 10 different training random seeds.

variations in the parameters of the cart dynamics (in fact, in the above example we are multiplying both friction and mass of the cart by a factor of 3), but that if we drastically reduce the length and mass of the pendulum by a 50%, our method fails. We hypothesize that this might be related to the underactuated nature of the pendulum dynamics. An interesting direction for future work would therefore be to study under which conditions the original value function retains the CLF properties for a new set of dynamics.

D.2 A1 Quadruped

Here we provide additional details of the A1 velocity tracking experiments detailed in Section 4. We use the locomotion controller presented in [19, Section 3.2] as our nominal baseline controller. This controller uses a linearized rigid-body model to formulate a quadratic-program (QP)-based controller to track a desired body pose of the robot. Specifically, the following QP is solved to obtain the ground reaction forces f for the feet in contact with the ground:

$$\begin{aligned} \min_f \quad & \|\mathbf{M}f - \tilde{g} - \ddot{q}_d\|_Q + \|f\|_R \\ \text{s.t.} \quad & f_z \geq 0, \\ & -\mu f_z \leq f_x \leq \mu f_z, \\ & -\mu f_z \leq f_y \leq \mu f_z, \end{aligned} \quad (33)$$

where \mathbf{M} is the inverse inertia matrix of the rigid body, $\tilde{g} := [0, 0, g, 0, 0, 0]$ denotes the acceleration due to gravity and $\ddot{q}_d \in \mathbb{R}^6$ are the desired pose accelerations of the robot’s body. In particular, the desired accelerations are obtained using a PD controller,

$$\ddot{q}_d = -k_p(q - q_d) - k_d(\dot{q} - \dot{q}_d), \quad (34)$$

with $q \in \mathbb{R}^6$ denoting the robot’s body pose.

When the feedback gains $k_p, k_d \in \mathbb{R}^6$ are not well tuned, large tracking errors in the forward speed of the robot can persist as illustrated in Fig. 3. To compensate for the increased tracking error, we learn a policy π_θ (MLP with two hidden layers of size 32×32) that outputs an additional acceleration term in (34), making the final desired acceleration $\ddot{q}_d = -k_p(q - q_d) - k_d(\dot{q} - \dot{q}_d) + \pi_\theta$. π_θ can therefore be viewed as a learned fine-tuning policy with respect to a model-based controller. The observations for the RL agent include the forward and lateral velocity, the roll and pitch orientation and the desired forward velocity of the robot. The actions include offsets to the desired forward and lateral accelerations.

The policy π_θ is learned directly on the robot hardware using a CLF W designed for the nominal rigid body dynamics of the robot following the procedure described in [39]. For training, we use SAC [47] with the reward $r_k = \frac{(W(F(x_k, u_k)) - W(x_k))}{\Delta t_k} + \lambda \|u_k\|^2$. The CLF term in the reward allows us to use a discount factor $\gamma = 0$, which considerably reduces the complexity of the learning problem. Indeed, within only 5 minutes of data collected from the robot hardware, our method is able to significantly reduce the tracking error in the forward velocity compared to the nominal locomotion controller, as shown in Figure 3.

D.3 Inverted Pendulum

The states of the system are $x = (\theta, \dot{\theta}) \in \mathbb{R}^2$, where θ is the angle of the arm from the vertical position, and the input $u \in \mathbb{R}$ is the torque applied to the joint. In each of the reinforcement learning experiments reported in Section 4 for this system we sample initial conditions over the range $-\pi \leq \theta \leq \pi$ and $-0.1 < \dot{\theta} < 0.1$. We use the soft actor critic (SAC) algorithm [20] and each training epoch consisted of 5 episodes with 100 simulation steps each, where each time step for the simulator is 0.1 seconds. To determine whether a given controller stabilizes the system we randomly sample 20 initial conditions and see if each trajectory reaches the set $\{x \in \mathbb{R}^n : \|x\|_2 < 0.05\}$ within 20 seconds of simulation. In Figure 4 we compare training curves across experiments with different discount factors and costs, thus we normalize each training curve so that a reward of 0 indicates the average reward during the first epoch, while a reward of 1 is the largest average reward obtained across all epochs. On each training curve, the black dot indicates the first controller that was able to stabilize the system, using the method described above. For each scenario we swept across values of the discount factor in increments of 0.05 from $\gamma = 0$ to $\gamma = 0.95$ and also tried $\gamma = 0.99$.

First, we use a reward of the form $r_k = -[W(F(x_k, u_k)) - W(x_k)] - \|x_k\|_2^2 - 0.1\|u_k\|_2^2$ to train the learned controllers. For $|u| \leq 20$ we were able to learn a stabilizing controller with $\gamma = 0$, for $|u| \leq 7$ we were able to learn a stabilizing controller with $\gamma = 0.5$, and for $|u| = 4$ were able to learn a stabilizing controller with $\gamma = 0.95$. Training curves for each of the critical values of the discount factor are depicted in Figure 4 (a). Each curve indicates the average reward per epoch across 10 different training runs and reports the best results for each scenario after an extensive hyperparameter sweep. As predicted by our theoretical results, when $|u| \leq 20$ a stabilizing controller is learned very rapidly as W is a good CLF for this system, while the cases where $|u| \leq 7$ and $|u| \leq 4$ take longer to train. Moreover, we observe that larger discount factors are required when $|u| \leq 7$ and $|u| \leq 4$, as W becomes a poorer candidate CLF for these cases.

Next, we compare our approach to a more traditional reward of the form $r_k = -\|x_k\|_2^2 - 0.1\|u_k\|_2^2$, which is the previous reward with the CLF term removed. We again swept over different values of discount factors to approximately determine the critical value of the parameter which yields stabilizing control laws. For $|u| \leq 20$ we require $\gamma = 0.8$, for $|u| = 7$ we required $\gamma = 0.95$ and for $|u| = 4$ we required $\gamma = 0.99$ to stabilize the system. These critical values of the discount factor also corresponded to the experiments which most rapidly learned stabilizing controllers for the new reward. Training curves for these two cases are reported in Figure 4 (b). Comparing the two sets of training curves in Figure 4 we see that the addition of the CLF terms consistently decreases the amount of data that is needed to learn a stabilizing controller, even when W is not a global CLF for the system.